Magnetostriction of Spin Ice under High Magnetic Fields

Nan Tang[1], Masaki Gen[2]

1 Nakatsuji lab, Department of Advanced Materials, Graduate School of Frontier Sciences, Univ. of Tokyo

2 Kohama lab, Department of Applied Physics, Graduate School of Engineering, Univ. of Tokyo

Author Introduction

Nan Tang: Specializes in low-temperature thermodynamic measurements using dilution refrigerator. In this research, she synthesized the single crystalline $Pr_2Zr_2O_7$ using floating zone method and prepared the sample for the high-field experiments.

Masaki Gen: Specializes in high-field measurements. In this research, he performed magnetostriction measurements under high field.

Abstract

In frustrated magnets, geometrical frustration prevents long-range magnetic order and leads to exotic state of matter like spin liquid. Spin ice is such a state whose ground state do not show long-range order, but a short-range "2-in, 2-out" correlations instead. Local Ising anisotropy induced by the competition between crystal electric field (CEF) effect and magnetic interactions is crucial in order to form such spin-ice correlations. Nevertheless, a systematic study about this fundamental requirement is still lacking. Here, we performed magnetostriction measurements of classical spin ice $Ho_2Ti_2O_7$ and quantum spin ice candidate $Pr_2Zr_2O_7$ under high magnetic fields up to ~ 53 T to discover new phenomena beyond Ising limit. We observed that the magnetostriction $\Delta L/L$ of $Ho_2Ti_2O_7$ exhibits a broad hump around 35 T, while that of $Pr_2Zr_2O_7$ shrinks monotonically. Based on these observations, we discuss the role of crystal electric field effect and exchange-striction effect in driving the behavior of $\Delta L/L$.

1. Research Background and Motivation

Cubic pyrochlore oxides $R_2T_2O_7$, with R being a magnetic rare earth and T a transition-metal ion, are among the most intensively studied frustrated magnets. The R^{3+} and T^{4+} ions form two pyrochlore lattices, namely the network of corner-sharing tetrahedra (Fig. 1 (a)). The crystal electric field (CEF) effect induced by the surrounding oxygen ions leads to a strong local Ising anisotropy of the spins. Such local Ising anisotropy and its competition with magnetic interaction lead to a spin-liquid state where no long-range order is formed down to miliKelvin temperature range. A famous example of this kind is the "classical spin ice" in which the local ice rules lead to a "2-in, 2-out" arrangement where two spins point into and two spins point out of each tetrahedron. Such a spin configuration features a

macroscopic ground-state degeneracy with residual entropy [1]. Spin ice receives much attention not only due to its peculiar spin correlations, but also an exotic excitation known as the deconfined magnetic monopole that is generated in pair in the "3(1)-in, 1(3)-out" polarized state [2].

$Ho_2Ti_2O_7$ and $Dy_2Ti_2O_7$ are the two prototypical examples of the "classical spin ice" [3]. For the Pr-based pyrochlores $Pr_2T_2O_7$ (T= Zr, Hf, Sn) [4-7], a quantum version of spin-ice state, namely the "quantum spin ice" is highly likely to be realized. It is characterized by an infinite superposition of quantum-entangled "2-in,2 -out" configurations and hosts exotic excitations, such as the linearly dispersive gapless "photon", gapped "quantum monopoles", and "magnetic monopoles". The Ising anisotropy of a quantum spin ice state is weaker than that of its classical counterpart due to the presence of perturbative transverse exchange interaction. Nevertheless, the local Ising anisotropy is still crucial for realizing a quantum spin ice, while systematic investigation on this fundamental requirement is lacking.

Here, we performed magnetostriction measurements under high fields up to ~ 53 T on classical spin ice material $Ho_2Ti_2O_7$ and the quantum spin ice candidate $Pr_2Zr_2O_7$. The magnetostriction, namely the macroscopic lattice changes under magnetic fields, allows us to gain insight into the microscopic spin correlation. Moreover, comparison of our data with the high field magnetization result reported in [8] may reveal the strength of magnetoelastic coupling in these two materials. The magnetoelastic coupling plays an important role in frustrated systems, as frustration can be relieved by lattice distortion. Measuring magnetostriction under high fields on spin ice materials may enable us to discover new phenomena beyond Ising limit.

2. Experimental Method

■ Single crystal growth

Single crystals of $Pr_2Zr_2O_7$ were grown from polycrystalline feed rods using a high temperature Xenon type optical floating zone furnace (Crystal Systems Co., model: FZ-T-12000-X-VPS-B) at ISSP, University of Tokyo, following the same procedure described in the past study [1]. This method is called the floating zone method and its schematic diagram is shown in Fig. 1 (b). The photograph of $Pr_2Zr_2O_7$ during the actual growth is shown in Fig. 1(c). The important parameters during the floating zone growth are given in Table 1. After the growth, the samples are aligned to the [111] direction using the backscattering Laue X-ray diffractometer (Photonic Science) prior to the measurements (Fig. 1 (d)(e)). The samples are cut to the desired cuboid shape using crystal cutting machine equipped with diamond blade (CU-02, Crystal Systems Corporation).

Ar-H_2 flow rate	0.2 L/min
Pulling down rate	Feed: 19 mm/h Seed: 19 mm/h
Rotation	Feed: 10 rpm, clockwise Seed: 10 rpm, counterclockwise
Xe lamps	3 kW × 4 ON
Melting start	~14 % power
Connect two rods	25~30 % power

Table 1: Important parameters during the single crystal growth.

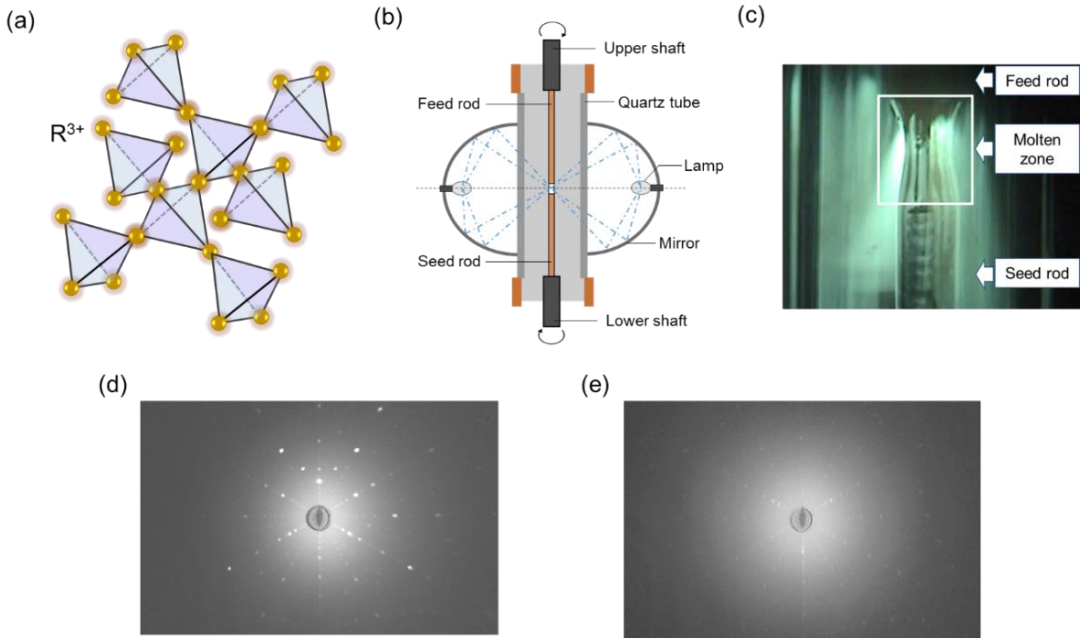

Figure 1 : Single crystalline growth of $Pr_2Zr_2O_7$ and $Ho_2Ti_2O_7$. (a) Pyrochlore lattice. (b) Schematic diagram of optical floating zone apparatus. The feed/seed rod is set in the upper/lower shaft respectively. The quartz tube is put outside of these rods, allowing a vacuum or (e.g.) an Ar gas atmosphere inside the tube. The lamps are placed inside the well-designed ellipsoidal mirrors. The light from the lamps (blue dashed lines) reflects on these mirrors and is eventually focused on the center of the sample space. The temperature of this focal point can reach 2000 ~ 3000 ℃. The tips of the two rods are melted into liquid at this focal point, and are called molten zone or floating zone. The two shafts rotate at opposite directions in order to mix the molten zone well. (c) Photograph of $Pr_2Zr_2O_7$ during the actual growth. (d) Laue X-ray photo of single crystalline $Ho_2Ti_2O_7$ along the [111] direction. (e) Laue X-ray photo of single crystalline $Pr_2Zr_2O_7$ along the [111] direction.

■ Magnetostriction measurement under high magnetic fields

Magnetostriction is measured using "Fiber Bragg Grating (FBG)" method (Fig. 2(a)). FBG is an optical fiber with a Bragg grating placed at the fiber core. The Bragg grating is formed by the modulation of the refractive index of the fiber core in the axial direction. Light with a Bragg wavelength $\lambda_B = 2nd$ is reflected back by the Bragg grating, where n and d are the refractive index and period of the Bragg grating, respectively. The change in the length ΔL of the FBG is in proportion to $\Delta\lambda_B$, the shift of λ_B. Thus, $\Delta L/L$ of materials coupled with the FBG can be measured by monitoring $\Delta\lambda_B/\lambda_B$. The decrease (increase) of reflected intensity corresponds to the increase (decrease) of $\Delta L/L$. FBG method is immune to electromagnetic and mechanical noise and does not require calibration, leading to a resolution of $\Delta L/L \sim 10^{-7}$. The single crystal sample is mounted on a soft clay, attached to the optical fiber.

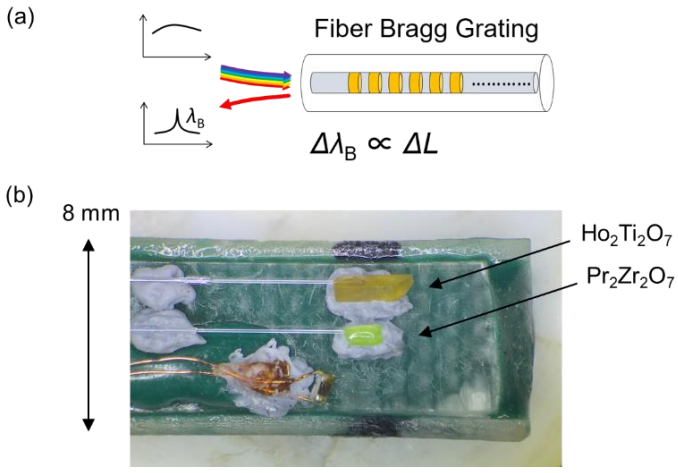

Figure 2 : Magnetostriction measurement of single crystalline samples $Pr_2Zr_2O_7$ and $Ho_2Ti_2O_7$. (a) Schematic diagram of Fiber Bragg Grating (FBG) method. (b) Sample mounting of $Pr_2Zr_2O_7$ and $Ho_2Ti_2O_7$.

3. Results and Discussions

Figure 3 shows the temperature (T) dependences of the inverse magnetic susceptibility (χ^{-1}) for $Ho_2Ti_2O_7$ and $Pr_2Zr_2O_7$ measured at B = 0.1 T. As shown in Fig. 3 (a), χ^{-1} follows Curie-Weiss law between 16 – 40 K, yielding a Curie-Weiss temperature θ_{CW}= 1.4 K and an effective magnetic moment $\mu_{eff} = 10.4\,\mu_B$ for $Ho_2Ti_2O_7$. Below 10 K, χ^{-1} deviates from the Curie-Weiss law. This behavior is consistent with the previous study [3, 11]. The positive θ_{CW} value indicates a ferromagnetic exchange interaction, and is at the same order (~ K) with magnetic dipole-dipole interaction in spin ice materials [3]. Similarly, for $Pr_2Zr_2O_7$, we obtain $\theta_{CW} = -0.62$ K and $\mu_{eff} = 2.78\,\mu_B$ within the fitting range of 2-10 K, which is again consistent with the previously reported values [4, 5].

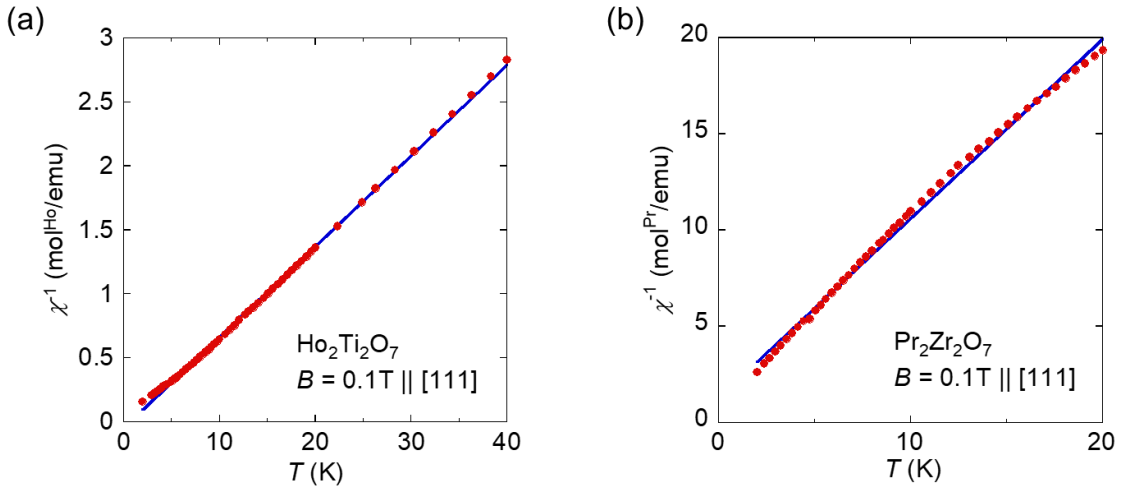

Figure 3 : Temperature (T) dependences of inverse magnetic susceptibility (χ^{-1}) for (a) $Ho_2Ti_2O_7$ and (b) $Pr_2Zr_2O_7$ measured at B= 0.1 T. The red dots are experimental data taken at zero-field-cooled condition. The blue line is a Curie-Weiss fit from 2-40 K for (a) $Ho_2Ti_2O_7$ and 2-20 K for (b) $Pr_2Zr_2O_7$.

Figure 4 (a) shows the normalized reflected intensity of the fiber attached to the $Ho_2Ti_2O_7$ or $Pr_2Zr_2O_7$ sample under one magnetic field pulse as a function of time t (ms). This reflected intensity is proportional to the change of the wavelength $\Delta\lambda_B/\lambda_B$, and thus can be directly converted to the magnetostriction $\Delta L/L$ of the sample studied**.** The magnetic field (B) dependences of magnetostriction $\Delta L/L$ for both samples $Ho_2Ti_2O_7$ and $Pr_2Zr_2O_7$ under the configuration $B//\Delta L//[111]$ at 4.2 K are shown in Fig. 4 (c) and 4 (d). The red (blue) curve corresponds to up (down) field scan. The hysteresis between up and down scans is reproduced even with two different optical systems. Therefore, the possibility from the measurement system itself can be excluded. Here, there are three possible reasons for this hysteresis: 1) Sample's magnetocaloric effect makes the temperature higher during the up-sweep scan compare to that of down-sweep scan. 2) Spin relaxation is different between up/down field scan. 3) The sample is not perfectly glued to the sample stage, thus might move from the initial position during down-field scan. For $Ho_2Ti_2O_7$, all three causes are possible, hence we might need further experiment to confirm if the hysteresis is an intrinsic feature of the sample. For $Pr_2Zr_2O_7$, 1) Sample's magnetocaloric effect is highly likely to be the cause of the hysteresis.

For $Ho_2Ti_2O_7$, $\Delta L/L$ expands up to ~ 35 T and shrinks gradually with a further increasing magnetic field, resulting in a broad hump at ~ 35 T. At 50 T, $\Delta L/L$ becomes smaller than that of zero field. First of all, our data in the low-field range below 5 T shown in Fig. 4 (c) is both quantitively and qualitatively consistent with that reported in [12] that shows an expanding $\Delta L/L$ on the order of 1×10^{-5} amplitude up to 5 T, measured by capacitance dilatometer under steady-state magnetic fields. This consistency ensures the reliability of our high field measurements. Secondly, the hump locates at around 35 T, which corresponds to ~ 24 K, while the first excited state is more than 200 K above the

ground state doublet. Thus, the crystal electric field effect cannot explain this broad hump. We might need further experiments to confirm if this hump is an intrinsic feature. Thirdly, in Ref. [8], B dependence of magnetization (M) of $Ho_2Ti_2O_7$ shows a step-like increase from 50 to 60 T for field applied along [5513] direction. Such anomaly is not observed in $\Delta L/L$ for field applied along [111] direction. Measuring magnetization at [111] direction can help us to gain insight about the strength of magnetoelastic coupling in $Ho_2Ti_2O_7$.

For $Pr_2Zr_2O_7$, the lattice shrinks monotonically down to 53 T, without exhibiting any sharp kinks or peaks (Fig. 4 (d)), indicating the lacks of field-induced phase transition up to 53 T. The first excited CEF level is ~ 108 K above the ground state doublet, and therefore the mixing of the CEF levels cannot occur below 53T, which is equivalent to 36 K. We then conclude that the monotonic decrease of $\Delta L/L$ is mainly caused by the exchange-striction effect. Namely, the exchange interactions between spins are dependent on the relative position of the ions, thereby coupling the spin configuration to the lattice structure. Again, the low field data of Fig. 4 (d) is quantitatively and qualitatively consistent with the magnetostriction data measured using capacitance dilatometer equipped in a steady-state superconducting magnet shown in Fig. 4 (b).

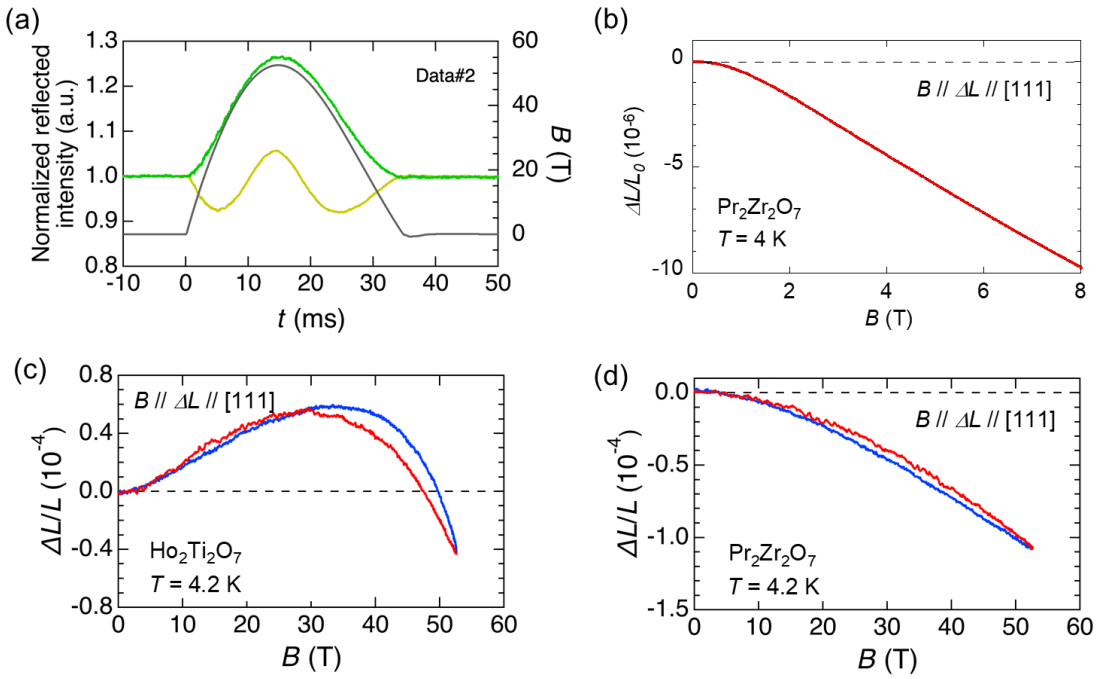

Figure 4 : Magnetic field (B) dependence of magnetostriction ($\Delta L/L$) for $Ho_2Ti_2O_7$ and $Pr_2Zr_2O_7$ at T= 4.2 K under $B//[111]$. (a) The green (yellow) curve is the normalized reflected intensity (right axis) of the fiber attached to $Ho_2Ti_2O_7$ ($Pr_2Zr_2O_7$) under one pulsed field with respect to time t (ms). The gray curve represents magnetic field (right axis) with respect to time t (ms). (b) B dependence of $\Delta L/L$ for $Ho_2Ti_2O_7$ along the [111] direction. (c) B dependence of $\Delta L/L$ for $Pr_2Zr_2O_7$ along the [111] direction. The red (blue) curve represents up (down) field sweep.

4. Conclusions and Future Prospect

In this study, we successfully grew single crystals of quantum spin ice candidate material $Pr_2Zr_2O_7$, and performed high-field magnetostriction measurement for the configuration $B//\Delta L//[111]$ up to 53 T for both $Pr_2Zr_2O_7$ and $Ho_2Ti_2O_7$. The low field part of both data is consistent with magnetostriction measurement using a steady-state superconducting magnet. We observed a broad hump in $\Delta L/L$ for $Ho_2Ti_2O_7$, whose origin is mysterious. In contrast, $\Delta L/L$ for $Pr_2Zr_2O_7$ shows a monotonic decrease, whose main contribution is possibly due to the exchange-striction mechanism. For future work, further experiments are needed to confirm if the broad hump of in $\Delta L/L$ for $Ho_2Ti_2O_7$ is true. Moreover, a detailed calculation is necessary to uncover the strength and roles of magnetoelastic coupling in shaping spin ice states.

Acknowledgement

We would like to acknowledge Prof. Satoru Nakatsuji from Department of Physics, Graduate School of Sciences, and Prof. Yoshimitsu Kohama from Deparment of Applied Physics, Graduate School of Engineering for providing tremendous support to proceed this research. Dr. Mingxuan Fu from Department of Physics, Graduate School of Sciences, has given a lot of helpful advice. The single crystal sample of $Ho_2Ti_2O_7$ is provided by Prof. Kazuyuki Matsuhira from Kyushu Institute of Technology. Regarding the single crystal growth of $Pr_2Zr_2O_7$, Dr. Kenta Kimura from Department of Advanced Materials, Graduate School of Frontier Sciences and Dr. Rieko Ishii from Institute for Solid State Physics (ISSP) have given tremendous support. We would also like to appreciate the MERIT advisor, Prof. Yukitoshi Motome MERIT for giving the permission to proceed the research. In the end, we would like to express our sincere gratitude to all the staff member of MERIT program.

References

[1] A.P. Ramirez *et al.*, Nature **399**, 333-335 (1999).

[2] C. Castelnovo *et al.*, Nature **451**, 42-45 (2008).

[3] S.T. Bramwell and M.J.P Gingras, Science **294**, 1495-1501 (2001).

[4] K. Kimura *et al.*, Nat. Commun. **4**, 1934 (2013).

[5] S. Petit *et al.*, Phys. Rev. B **94**, 165153 (2016).

[6] R. Sibillie *et al.*, Nat. Phys. **14**, 711-715 (2018).

[7] H. D. Zhou *et al.*, Phys. Rev. Lett. **101**, 227204 (2008).

[8] L. Opherden, *et al.*, Phys. Rev. B **99**, 085132 (2019).

[9] N. Tang, master thesis (2018).

[10] A. Ikeda *et al.*, Rev. Sci. Instrum. **88**, 083906 (2017).

[11] K. Matsuhira *et al.*, J. Phys.: Condens. Matter **12**, L649–L656 (2000).

[12] T. Stoter, PhD dissertation (2019).